



# Novel pneumatically assisted atomization device for living cell delivery: application of sprayed mesenchymal stem cells for skin regeneration

Lixing Zhang<sup>1,2</sup> · Xintao Yan<sup>1,4</sup> · Li An<sup>1</sup> · Meijia Wang<sup>1</sup> · Xi Xu<sup>1</sup> · Zhonglin Ma<sup>1</sup> · Mengting Nie<sup>1</sup> · Fangzhou Du<sup>1</sup> · Jingzhong Zhang<sup>1,2,3</sup> · Shuang Yu<sup>1,2,3</sup>

Received: 18 March 2021 / Accepted: 9 June 2021 / Published online: 21 July 2021  
© Zhejiang University Press 2021

## Abstract

Large cutaneous wounds pose a severe medical problem and may be deadly in cases when regeneration is impaired. Recently, topical stem cell therapy has been realized as a promising strategy for wound healing and skin regeneration. However, stem cells must be administrated uniformly to the wound area, otherwise treatment will be ineffective, which has been a limitation of current administration methods. Specifically, the delivery pressure and nozzle features of most clinical cell spray devices are unknown, which may significantly affect the viability of sprayed cells and their capacity for proliferation. Herein, we developed a novel pneumatically assisted atomization device (PAAD) in which cell suspensions were uniformly atomized at a low delivery pressure. We optimized the applied fluidic pressure and air pressure to maximize cell survival and function for the application of multiple cell types, while ensuring uniform dispersal across the wound site. Moreover, we found that the application of sprayed umbilical cord-derived mesenchymal stem cells to wound sites significantly accelerated wound healing and promoted appendage regeneration on an excisional cutaneous wound model. Overall, the novel PAAD system delivered living cells uniformly and maintained the viability and differentiation of sprayed cells, strongly suggesting its potential for application in clinical cell therapy, especially for large, irregular, and severe skin wounds.

**Keywords** Cell delivery · Skin wound · Wound healing · Spray application · Cell-spray autografting · Stem cell therapy

## Introduction

Impaired wound healing is not only a major global health problem [1], but also imposes a huge economic burden worldwide [2]. Serious and large skin wounds, most notably

incurred as a result of accidental cuts, burns, and chronic refractory skin ulcers are plagued by slow healing, are prone to infection, and often form hypertrophic scars [3].

Stem cell therapy is a promising approach for the treatment of non-healing wounds [4]. In recent years, various forms of stem cell therapy have been applied in preclinical and clinical trials to evaluate their impact on wound healing [5]. Mesenchymal stem cells (MSCs) isolated from bone marrow, adipose tissue, the umbilical cord, and umbilical cord blood [6] were all demonstrated to promote wound healing in several animal models and in clinical trials, with the advantages of low immunogenicity, high proliferation rates, and excellent safety [7–9]. Previous reports showed that MSCs could promote the functional recovery of patients during wound healing by recruiting cells, cytokines, matrix proteins [10, 11], and by exerting paracrine effects [12–14].

It has been well-established that the method of cell administration can significantly affect the distribution of cells in the wound [15, 16]. Although any of intravenous, intramuscular, or topical administration of MSCs into mice

---

Lixing Zhang and Xintao Yan have contributed equally to this work.

✉ Jingzhong Zhang  
zhangjz@sibet.ac.cn

✉ Shuang Yu  
yush@sibet.ac.cn

<sup>1</sup> Suzhou Institute of Biomedical Engineering and Technology, Chinese Academy of Sciences, Suzhou 215163, China

<sup>2</sup> Zhengzhou Institute of Engineering and Technology Affiliated with SIBET, Zhengzhou 450001, China

<sup>3</sup> Xuzhou Medical University, Xuzhou 221004, China

<sup>4</sup> Academy for Engineering and Technology, Fudan University, Shanghai 200433, China

with a full-thickness wound achieved therapeutic effects, the two former administration methods were both found to result in poor concentration of stem cells in the wound sites [17]. In fact, topical application over the wound shortens treatment time and incurs less pain for patients. However, topical cell delivery by pipette or syringe is inefficient and uneven [18].

A more recent technique of cell-spray autografting by atomization of cell suspensions has enabled rapid cell delivery and enhanced wound re-epithelialization, particularly for patients with deep, large, and irregular wounds [19]. To our knowledge, the first automated device for cell suspension atomization was a pump-action aerosol nozzle designed to spray cells *in vitro* [20]. Several other types of spray devices have been subsequently designed, especially for applications involving tissue repair and regeneration [21], including air-brush pistols [22, 23], atomizers [24], or spray nozzles [25]. However, these devices proved to have several shortcomings limiting their effectiveness in wound healing. Most notably, a number of previously reported spray devices produce inconsistently atomized, nonuniform large droplets that are not evenly distributed within the wound [26]. Moreover, for most spray devices used in clinical practice, the delivery pressure and nozzle features are unclear, or cannot be precisely controlled [27]. For example, in a report on air-brush pistols, cell viability was only 65% at a delivery pressure of 69 kPa [20]. In a report by Fredriksson et al., cell viability was about only 45% 4 days after atomized application [28]. In short, most of the previously reported spray devices are not ideal for the delivery of living cells, which results in significantly impaired viability and proliferation of the sprayed cells.

In the present study, we designed a novel pneumatically assisted atomization device (PAAD) to improve the spraying process by systematically addressing issues of uniformity and distribution. The device can provide uniform droplets at a low air pressure, which facilitates the retention of cell viability, proliferation, and lineage differentiation after spray application. We tested this device at different air flow and fluidic pressures to obtain an optimal balance between cell viability and atomization uniformity. The cell suspension droplets were uniform at 70 kPa air pressure and 47.79 kPa fluid pressure, with no significant adverse impacts observed on viability, differentiation, or organoid formation ability of stem cells. Moreover, using fluorescence microscopy and an animal model for skin wounds, we demonstrated that the sprayed UC-MSCs could efficiently promote wound closure, re-epithelialization, and skin appendage regeneration *in vivo*. Therefore, this novel PAAD that is capable of delivering cells efficiently and uniformly to wound sites represents a promising tool for cell therapy, especially for large-area, irregular, and severe skin wounds.

## Materials and methods

### PAAD design and setup

The proposed pneumatically assisted atomization device (PAAD) was set up according to the schematic shown in Fig. 1. An oil-free air compressor (Shanghai Greeley Industrial Co. Ltd, China) was selected as the air source to provide gas pressure in the 0–100 kPa range. The gas pressure was accurately regulated by a barometric regulator (Airtrol Components Inc., USA). The nozzle parts of the PAAD were designed using Unigraphics NX software (Siemens Industry Software Inc., USA) to ensure that fluid was mixed with gas at the nozzle. The cell preparation was loaded into a 5 mL sterile Ruhr joint syringe (Shanghai Kindly Enterprise Development Group Co., Ltd., China) with a 27G needle (MUSASHI, Japan) and the syringe was pushed by a propeller precisely controlled by a proprietary stepper motor (Shinano Kenshi Co., Ltd., Japan). Air flow at setting pressure was mixed with the cell suspension at a speed of 5 mL/min in the nozzle, resulting in a regular interruption of fluid flow, thereby producing uniform atomized droplets. The nozzle diameter of the spray device was 0.8 to 1.0 mm, the spray cone angle was kept constant at 80°–90°, and the spray height was set to 10 cm.

### Measurement of atomization efficiency

According to the Hagen–Poiseuille equation, the liquid flow pressure was calculated as follows:

$$\Delta P = \frac{2.133\mu l Q}{\pi d^4},$$

where  $\Delta P$  = pressure difference between both ends of the needle (kPa);  $\mu$  = viscosity (Pa.s);  $l$  = length of needle (mm);  $Q$  = jet flow, ( $\text{mm}^3 \cdot \text{s}^{-1}$ );  $d$  = inner diameter of needle (mm).

We tested the flow volume and flow pressure at different settings, and compared the effects of different flow pressure on jet flow volume. We then checked the uniformity of the sprayed droplets using a laser diffraction particle size analyzer (JL-3000, JNGX, China). A 27G needle was used to inject ionized water at a flow rate of 5 mL/min, and testing was performed under airflow pressures of 40, 50, 60, 70, 80, 90, and 100 kPa. The monochromatic light of the laser beam could be strongly diffracted by each droplet of the atomized liquid, and a photomultiplier was used to record differences in signal pattern and intensity. These results were then populated into a particle size distribution chart. The R-R (Rosin–Rammler) distribution is often used to describe the continuous distribution of atomized particles, which can be calculated as follows:

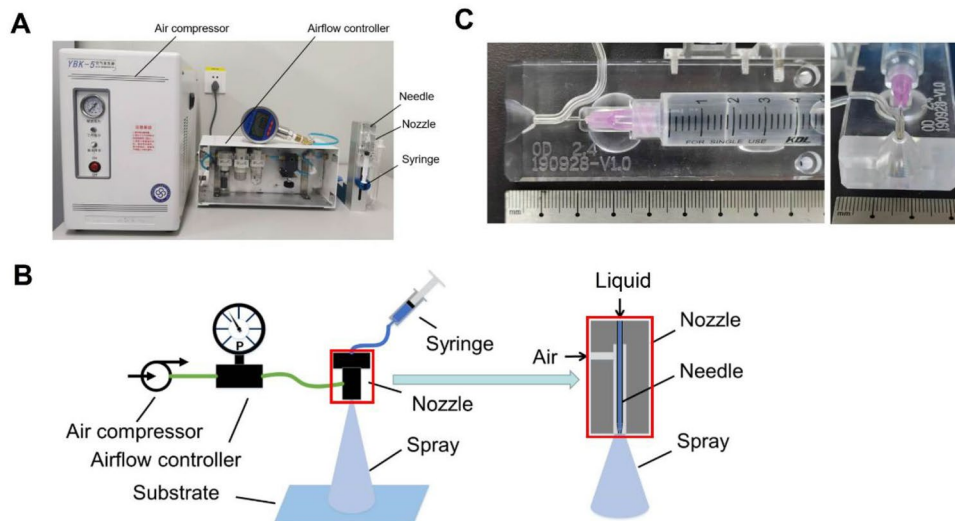


**Fig. 1** Pneumatically assisted atomization device and spray nozzle. **a** The exterior components of the pneumatically assisted atomization device (PAAD). **b** Schematic of the atomization system, which uses two-phase nozzles for uniform atomization of cell suspensions. An airflow controller ensures stable air pressure to the gas inlet of the

nozzle; a consistent flow of cell suspension is driven by positive pressure (such as a syringe pump) to the needle inlet on the nozzle. The red square shows a cross-sectional view of a two-phase flow atomizing nozzle. **c** Clear images about the core part of nozzle by horizontal and vertical ways

$$R_i = 1 - \exp \left[ - \left( \frac{d_i}{C} \right)^k \right],$$

where  $d_i$  = median particle size, which is the corresponding particle size value when the cumulative volume distribution percentage reaches  $i$  %;  $R_i$  represents the percentage of particles when the particle size is less than  $d_i$ .

The uniformity coefficient  $k$ , which is positively correlated with the atomization uniformity, was compared at different air influx rates using the following calculation:

$$k[d_1, d_2] = \frac{1}{\lg d_1 - \lg d_2} \left( \lg \ln \frac{1}{1 - R_1} - \lg \ln \frac{1}{1 - R_2} \right).$$

We further compared the homogeneity of cells applied by either a traditional pipette or the PAAD. Cells were stained with 4',6-diamidino-2-phenylindole (DAPI, Beyotime, China) for 15 min, followed by spraying 1 mL of cell suspension onto culture dishes using a syringe (1 mL, 0.4 × 13 RWLB, MSW, Shanghai, China) or the PAAD. The homogeneity of cells was also checked when the PAAD was loaded with different starting volumes. Bright field and fluorescence images were captured using an inverted fluorescence NIB900 microscope (Nexcope, Ningbo Yongxin Optical Co., Ltd., Ningbo, China).

### Isolation and cultivation of UC-MSCs

All tests were performed in accordance with the 'Ethical Guiding Principles on Human Embryonic Stem Cell

Research' (laid down by the Ministry of Science and Technology and the Ministry of Health, People's Republic of China, 2003) and the Declaration of Helsinki. Umbilical cords were generously donated by five mothers who had delivered healthy babies by cesarean section and had signed the informed consent with ethical approval from The First Affiliated Hospital of Soochow University, Jiangsu, China. The UC-MSCs were isolated and cultured *ex vivo* as previously described by Hu et al. [29]. Briefly, the umbilical cord vessels and outer membrane were removed and the mesenchymal tissue in Wharton's jelly was dissected and minced into 1 cm<sup>3</sup> pieces. These were inoculated into 10-cm diameter culture dishes with DMEM/F12 medium (C11330500BT, Gibco, USA) containing 10% fetal bovine serum (FBS, Gibco) and 1% penicillin–streptomycin. Half of the medium was replaced on the third day, and the total volume of medium was replaced every 3 days. The tissue blocks were removed when cells reached 50% confluence. The experiments for this study were performed using UC-MSCs cultured for 8 or fewer passages.

### UC-MSCs differentiation assays

The adipogenic and osteogenic differentiation of UC-MSCs were evaluated by Oil Red O and Alizarin Red Staining, respectively. The UC-MSCs were cultured with either MesenCult™ Adipogenic Differentiation Medium (05,412, Stemcell Technologies, Canada) or OriCell™ Osteogenic Differentiation Kit (HUXMA-90021, Cyagen, USA). For the adipogenic differentiation of UC-MSCs, cells were assessed

on day 14 by qualitative Oil Red O staining for lipid-filled mature adipocytes (C37A00150, VivaCell Biosciences, China). The Oil Red O stained lipid droplets were eluted with isopropanol, and the absorbance value was determined at 490 nm. The osteogenic differentiation of UC-MSCs was assessed on day 21 using Alizarin Red Staining for calcium nodules in mature osteocytes (C37C00150, VivaCell Biosciences). Subsequently, 10 M sodium phosphate was added to each well and the absorbance of the supernatant was determined at 490 nm. Images were acquired using an inverted NIB410 microscope (Nexcope).

### Primary skin epidermal cell isolation and organoid formation assay

Epidermal cells were isolated from the back skin of 8–16-week-old BALB/c mice as previously described [30]. For the epidermal organoid formation assays,  $1 \times 10^4$  cells were resuspended in 30  $\mu$ L reduced growth factor BME (Cultrex) and cultured in medium consisting of advanced DMEM/F12 (Gibco) supplemented with penicillin–streptomycin (100 U/L; Gibco), B27 supplement (50 $\times$  stock; Gibco), N-Acetylcysteine-1 (1 mM; Sigma-Aldrich, Germany), EGF (50 ng/mL, Invitrogen, USA), Noggin (100 ng/mL, Sino Biological, China), R-spondin (500 ng/mL, Sino Biological), Forskolin (10 ng/mL; Tocris, UK), A-83-01 (2  $\mu$ M; Tocris), and Rho kinase inhibitor Y-27632 (10  $\mu$ M; Sigma-Aldrich). The culture medium was refreshed every 3–4 days [31]. Images were acquired using an inverted NIB900 microscope (Nexcope). The formed organoids were measured and analyzed using ImageJ software (Version 2, National Institutes of Health, Bethesda, MD, USA).

### Cell viability assays

The cells were cultured with DMEM/F12 (C11330500BT, Gibco) medium containing 10% FBS (SV30087.03, Gibco) in T25 cm<sup>2</sup> or T75 cm<sup>2</sup> flasks. Cells were collected using trypsin when reaching 90% confluence, and the cell density was adjusted to 10<sup>6</sup> cells/mL. Half of the dissociated cells were used as the unsprayed control (unsprayed cells), and the other half were sprayed by PAAD (sprayed cells). To assess the ratio of live/dead cells following the spray application, both sprayed and unsprayed UC-MSCs were stained with trypan blue. The ratio of live/dead cells was calculated by the CountStar software (Ruiyu Biotech, China) based on the number of all cells and blue colored dead cells. Next, the viability of sprayed and unsprayed UC-MSCs was tested using a Cell Counting Kit-8 (CKO4, DOJINDO, USA) at 3, 24, and 48 h post inoculation. In addition, sprayed/unsprayed UC-MSCs and primary epidermal cells were cultured for the specified time periods and stained with Calcein-AM/PI LIVE/DEAD™ Viability/Cytotoxicity Kit (40747ES76,

YEASEN, China) for 15 min at 37 °C. Fluorescent images were captured and analyzed using a Nexcope inverted fluorescence microscope.

### Animal wound model preparation and transplantation experiments

All animal procedures were conducted in accordance with the guidelines of the Animal Welfare Committee of Suzhou Institute of Biomedical Engineering and Technology, Chinese Academy of Sciences (SIBET, CAS). 8–16-week-old BALB/c mice (20–23 g) were obtained from the animal facility of SIBET, CAS. An excisional wound model was generated on the backs of mice as previously reported [15]. In brief, after the removal of fur, two full-thickness 8 mm diameter excisional wounds were made on the back of each mouse using a biopsy punch. The animals were then randomly divided into three groups. To test cell function after spray application *in vivo*,  $1 \times 10^6$  dissociated UC-MSCs were sprayed through PAAD ('sprayed') or  $1 \times 10^6$  dissociated UC-MSCs ('unsprayed') were resuspended in 20  $\mu$ L 50% PBS/Matrigel (356231, Corning, USA) and applied onto each wound, which were then covered with a transparent antibacterial wound dressing (3 M, Germany). The 50% PBS/Matrigel alone served as the control treatment. Images of the wound areas were taken at day 0, 3, 7, 10, 14, 18, and 23 post-treatment. The wound margins were marked in the images, and the wound sizes were measured and analyzed using Analyser Software (Image J).

### Histology and immunofluorescence

The mice were sacrificed at the designated time points, and samples of skin containing the inflicted wound and the adjacent area were dissected and fixed with 4% paraformaldehyde overnight at 4 °C, and subsequently processed for paraffin embedding. Tissue sections were deparaffinized, rehydrated through graded ethanol solutions, and stained with hematoxylin and eosin. For Masson trichrome staining, sections were dyed with hematoxylin, acid Ponceau Fuchsin, and aniline blue to visualize collagen fibers and myofibers. Immunofluorescence staining was performed by incubating tissue sections with rabbit anti-cytokeratin 14 (Abcam), and visualized with Alexa 488-conjugated donkey anti rabbit antibody (Abcam). DAPI was employed for counterstaining nuclei. Images were captured using DMetrix widefield microscopy or a Leica TCS SP5 confocal microscope.

### Statistical analysis

Numerical data were expressed as means  $\pm$  SD. Data were subjected to 2-tailed Student's *t* tests or one-way ANOVA using GraphPad Prism 6.0 (GraphPad Software Inc., San

Diego, CA, USA) to evaluate differences between treatment groups. The asterisk was used to denote  $p < 0.05$  and ns to indicate that the difference was not significant.

## Results

### The development of a novel pneumatically assisted atomization device (PAAD)

We designed an atomization device that can administer cells quickly and evenly across the surface of a cell culture dish while retaining good cell viability and capacity for differentiation. Uniform cell dispersal is realized through pneumatically assisted atomization. As shown in Fig. 1a, the device consists of an air compressor, airflow controller, air jet pipe, cell reservoir, and circuit board. The cell suspension is impelled into the needle and driven by positive pressure to form a liquid stream at the nozzle outlet. The introduction of gas influx at a specific angle and pressure disrupts the liquid stream, resulting in the conversion of the continuous phase to a dispersed phase in which appropriately sized atomized droplets are formed for further application, such as wound healing (Fig. 1b). Clear images of the core part of nozzle in horizontal and vertical views are shown in Fig. 1c.

### Characterization of the PAAD

Hydraulic and gas pressure both affect cell viability and function, thus their appropriate settings provide the premise of atomization. The liquid flow pressure was measured with deionized water (Fig. 2a). Based on the Hagen–Poiseuille equation, we performed a linear regression and found that the coefficient for jet flow and hydraulic pressure was 99.53%, which exhibited a clear linear relationship between the fluid flow and hydraulic pressure (Fig. 2b). Accordingly, to obtain high flux atomization at 5 mL/min while ensuring a high cell survival rate, the hydraulic pressure was set to 47.79 kPa.

Next, we identified the influence of gas pressure on the atomization uniformity. Results showed that the narrower the size distribution of the sprayed droplets, the greater the uniformity of atomization. The distribution of equivalent particle size under different air pressures based on R–R (Rosin–Rammler) distribution is shown in Fig. S1A–S1G. The uniformity coefficient  $k$  value of D25 (which corresponded to the 25th percentile and below in the distribution of cumulative particle volumes, Fig. S2) and D75 (the particle size when the cumulative particle volume per total volume is 75%) were measured under gas pressures ranging from 40 to 100 kPa (Table 1). Based on the Rosin–Rammler particle size distribution function according to the formula described above, the results showed that the  $k$  values of D25 and D75 were positively correlated with the air pressure,

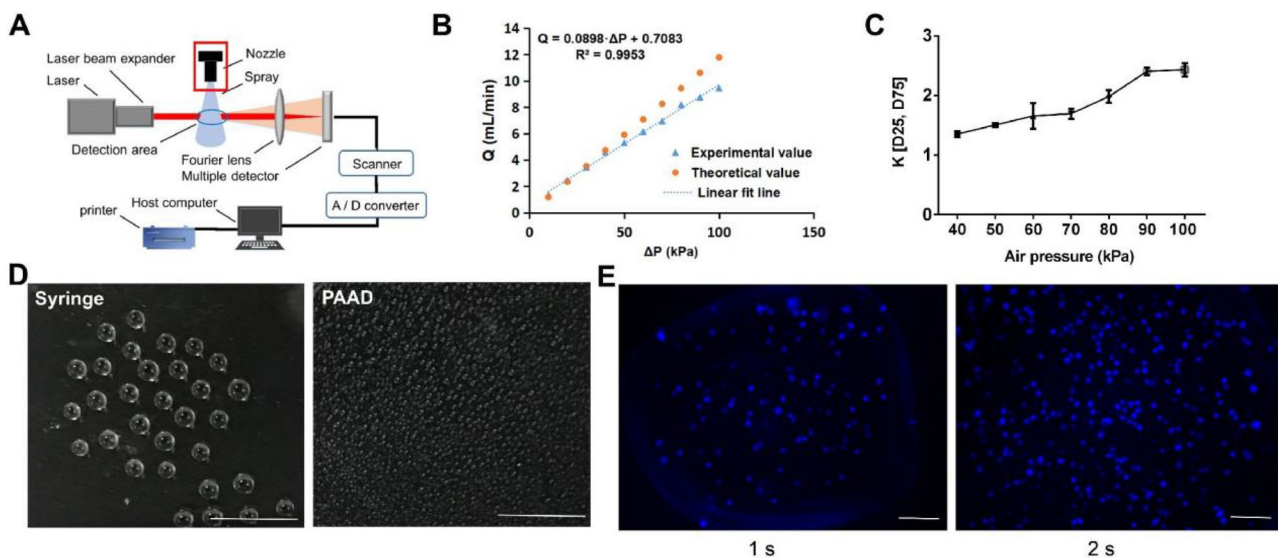


**Fig. 2** Characterization of the PAAD. **a** Schematic illustration of the method for measuring the size of atomized droplets of cell suspension. The size and uniformity of the sprayed droplets were checked using a laser particle size analyzer. **b** Linear regression analysis indicating a positive linear relationship between fluidic flow and hydraulic pressure. **c**  $k$  (D25, D75) values indicating that the coefficient of

atomization uniformity is positively correlated with air pressure. **d** Images of droplets delivered by Syringe (1 mL, 0.4 × 13 RWLB, left image) versus PAAD (right image). Scale bar: 1 cm. **e** Distribution of DAPI stained cells delivered by PAAD within 1 s and 2 s showing an increase in cell number with prolonged spraying time. Scale bar: 100  $\mu$ m. Numerical data represented as means  $\pm$  SD

**Table 1** Atomization uniformity coefficients under various pressures (mean  $\pm$  SD)

Pressure (kPa)	D25 ( $\mu\text{m}$ )	D75 ( $\mu\text{m}$ )	K [D25, D75]
40	231.47 $\pm$ 1.243%	744.39 $\pm$ 5.457%	1.35 $\pm$ 0.0161%
50	99 $\pm$ 3.53%	281.98 $\pm$ 1.158%	1.50 $\pm$ 0.0108%
60	59.86 $\pm$ 1.749%	159.78 $\pm$ 18.787%	1.66 $\pm$ 0.069%
70	52.428 $\pm$ 3.611%	133.03 $\pm$ 1.907%	1.69 $\pm$ 0.027%
80	48.6 $\pm$ 3.352%	107.89 $\pm$ 7.79%	1.98 $\pm$ 0.0331%
90	41.07 $\pm$ 6.776%	78.98 $\pm$ 7.38%	2.41 $\pm$ 0.0205%
100	39.5 $\pm$ 9.73%	75.37 $\pm$ 7.91%	2.43 $\pm$ 0.0362%

indicating that uniformity increased commensurately with air pressure.

In order to further check whether PAAD produced a more even and viable coating of cells than the commonly used administration methods, we sprayed 1 mL of cell suspension onto a culture surface using either a pipette or the PAAD (with air pressure at 70 kPa). Compared to the homogeneous droplets produced by PAAD application, the droplets squeezed through the syringe (1 mL, 0.4  $\times$  13 RWLB) were generally larger and had inconsistent sizes (Fig. 2d). Moreover, the uniformity achieved by PAAD was retained even with the increased duration of the spraying process, indicating that uniformity was not influenced by spray volume (Fig. 2e). Taken together, these results showed that, under hydraulic and air pressure settings that were considerably less than standard atmospheric pressure, the spray application using PAAD resulted in evenly and efficiently distributed cells.

### PAAD maintains cell viability and function

In order to test whether increasing airflow pressure adversely affects the viability of sprayed cells, the 293 T cells were sprayed at pressures of 50, 60, 70, 80, 90, and 100 kPa, for comparison with unsprayed cells as positive control. Trypan Blue staining was employed to examine the viability of sprayed cells immediately following application (Fig. 3a). The results of this assay showed no significant differences ( $p > 0.05$ ) in cell viability between unsprayed cells and those applied under air pressures from 50 to 80 kPa (Fig. 3b). However, at 90 and 100 kPa, cell viability significantly decreased to 90.69  $\pm$  2.5% and 89.07  $\pm$  2.3% ( $p < 0.01$ ), respectively, compared to controls. Next, the cells sprayed under air pressures between 50 and 100 kPa were cultured and cell growth was assessed using a cell counting kit-8 (cck-8) at 48 h postinoculation (hpi). Results showed that cell growth was negatively correlated with air pressure. As shown in Fig. 3c, when the spray air pressure increased from 70 to 80 kPa, cell growth reduced from 97.8  $\pm$  5.4% to 92.9  $\pm$  1.2%. Combining the data on atomization uniformity, cell viability and cell growth after spraying, 70 kPa was

selected to obtain uniform distribution and retain cell viability for further experiments.

Subsequently, we tested the long-term effects of atomization on epidermal stem cells and mesenchymal stem cells (MSCs), which are both used in cell therapy for wounds [5, 31]. For this test, epidermal stem cells freshly isolated from skin of adult mice and MSCs isolated from human umbilical cord were sprayed using PAAD at 70 kPa. Cell viability was determined using Calcein-AM/PI staining at 24 and 48 hpi (Fig. 4a and 4c), revealing that the ratio of live/dead cells was not significantly different between sprayed and unsprayed cells. Cell growth was further evaluated using a cell counting kit-8 (cck-8) to determine the rate of proliferation at 3, 24, and 48 hpi (Fig. 4b and 4d). For both freshly isolated epidermal stem cells and cultured MSCs, no significant differences in cell proliferation were observed between the sprayed and unsprayed cells throughout the 48 hpi. As a whole, these results showed that, at 70 kPa PAAD air pressure, both the viability and proliferative function of cells were well-maintained during the spraying process.

### Stem cells sprayed by PAAD retain the ability to form organoids and differentiate

Previous studies have shown that epidermal cells can form functional epidermal organoids in vitro, in which the basal–apical organization of the mouse epidermis is maintained [32]. Thus, we investigated whether primary epidermal cells applied by PAAD could retain their differentiation and organoid-forming functions after atomization, and subsequently found that their ability to form epidermal organoids was conserved (Fig. 5a). No significant differences ( $p > 0.05$ ) in the efficiency of organoid formation (Fig. 5b) or organoid area (Fig. 5c) were detected between sprayed and unsprayed epidermal cells.

In addition to, multipotent progenitor cells (UC-MSCs), which are capable of differentiating into osteoblastic or adipocytic lineages, were also tested for changes in their capacity to differentiate after spray application by PAAD (Fig. 5d and 5e). The ratio of UC-MSCs that differentiated into adipocytes, as indicated by the Oil Red O staining of lipids, showed no significant differences [(0.81  $\pm$  0.05) vs

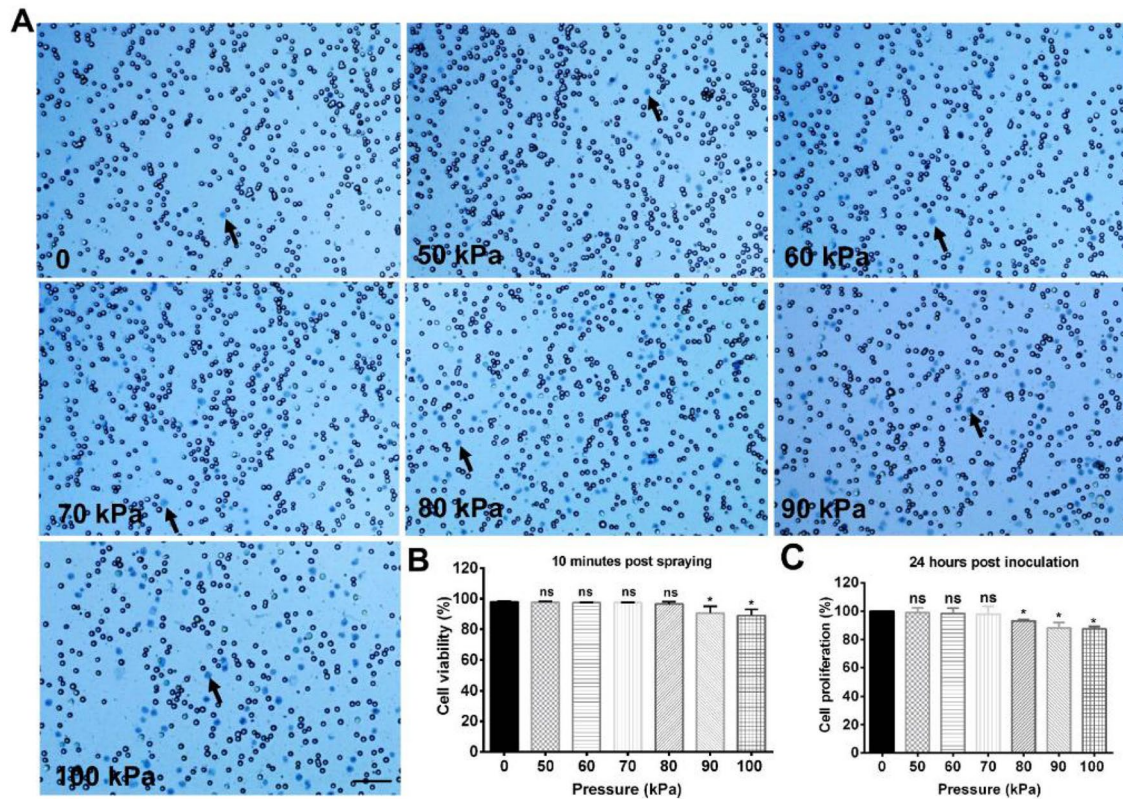


**Fig. 3** Viability of cells sprayed by PAAD. **a** 293 T cells were sprayed by PAAD at a range of air pressures including 50, 60, 70, 80, 90, and 100 kPa. Trypan blue staining shows the ratio of live/dead cells. Arrows indicate Trypan blue stained dead cells. **b** The viability

of sprayed cells was calculated by CountStar (Ruiyu Biotech) software. **c** The growth of sprayed cells was negatively correlated to air pressure. Numerical data represent means  $\pm$  SD. ns indicates  $p > 0.05$ , \* indicates  $p < 0.05$  versus the corresponding control

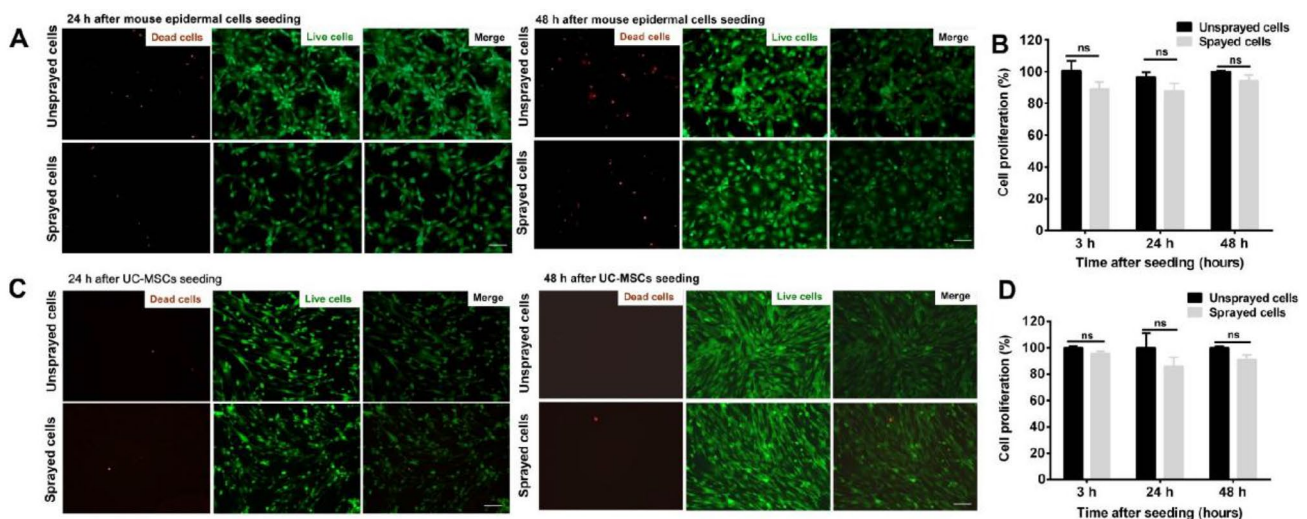


**Fig. 4** The proliferation of cells was not impaired by the PAAD spraying process. **a** Sprayed and unsprayed mouse epidermal cells were cultured for 24 and 48 h after cell seeding and stained with calcein-AM/PI to identify live (green) or dead (red) cells. **b** The proliferation of sprayed and unsprayed mouse epidermal cells showed no significant differences at 3, 24, or 48 h after cell seeding. **c** Sprayed

and unsprayed UC-MSCs were cultured for 24 and 48 h after cell seeding and stained with calcein-AM/PI to identify live (green) or dead (red) cells. **d** The proliferation of sprayed and unsprayed UC-MSCs showed no significant differences at 3, 24, or 48 h after cell seeding. Scale bar: 100  $\mu$ m. Numerical data represent means  $\pm$  SD. ns indicates  $p > 0.05$  versus the corresponding control

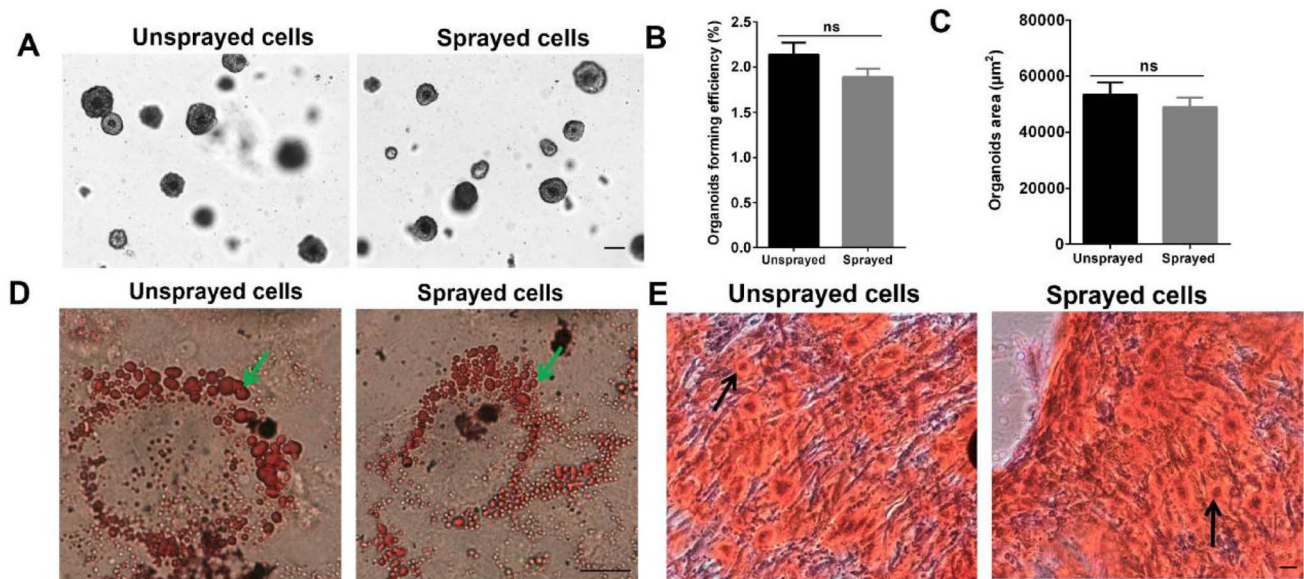


**Fig. 5** The ability to form organoids by sprayed mouse epidermal cells and the ability to differentiate into adipogenic/osteogenic lineages by sprayed UC-MSCs were retained during the spraying process. **a** Brightfield images of organoids derived from sprayed and unsprayed mouse epidermal cells (Scale bars: 100 µm). **b** No significant differences were observed in organoid-forming efficiency between the sprayed and the unsprayed mouse epidermal cells (Scale

bar: 100 µm). **c** Average size of organoids derived from sprayed mouse epidermal cells showed no difference from that of unsprayed cells. Sprayed UC-MSCs had similar capacity for adipogenic (**d**) and osteogenic (**e**) differentiation compared to unsprayed UC-MSCs. Green arrows indicate lipid droplets. Black arrows indicate calcium nodules. Scale bar: 20 µm. Numerical data represent means  $\pm$  SD. ns indicates  $p > 0.05$  versus the corresponding control

( $0.87 \pm 0.04$ ),  $p > 0.05$ ] between sprayed and unsprayed groups. In a similar manner, the ratio of UC-MSCs that differentiated into osteoblasts, as evidenced by alizarin red calcium staining, did not exhibit significant differences [( $1.93 \pm 0.07$ ) vs ( $2.12 \pm 0.11$ ),  $p > 0.05$ ] between sprayed and unsprayed groups. These results cumulatively showed that the functions of two different stem cell types were well-maintained after spraying by PAAD.

### UC-MSCs sprayed by PAAD maintain their ability to promote wound healing

Aiming to determine if PAAD could be applied as a clinical technique for wound treatment, we next investigated whether sprayed UC-MSCs preserve their capacity to heal excisional skin wound animal models in vivo. Using (BALB/c mouse line) mice, we established that the application of both sprayed and unsprayed UC-MSCs significantly reduced wound size over several time points compared to the control applications (Fig. 6a and 6b). Notably, the differences in wound size were significant until 10 days post-UC-MSCs administration.

During the process of wound healing, local fibroblasts secrete collagen and fibronectin, which comprise newly formed granulation tissue, and promote the recovery of the wound area [33]. MSCs play a major role in coordinating the repair response by recruiting other cells and matrix proteins.

To further assess whether sprayed UC-MSCs affect the cellular and molecular mechanisms associated with wound healing, we performed histological staining on skin tissue dissected from the wound sites at days 7 and 23 post-UC-MSCs application. The H&E staining showed thicker tissue layers, and well-formed granulation tissue were observed in the groups treated with sprayed and unsprayed cells than in the control group on day 7 after treatment (Fig. 6c). No significant differences ( $p > 0.05$ ) in wound length (Fig. 6d) and wound thickness (Fig. 6e) were observed between the sprayed and unsprayed groups, indicating that the sprayed hUC-MSCs maintained their ability to promote wound healing. Furthermore, Masson trichrome staining revealed greater collagen deposition in wounds treated with sprayed and unsprayed cells than in the control group at the same time point (Fig. 6f), indicating that PAAD spraying did not inhibit matrix protein recruitment by UC-MSCs.

The wounds were completely healed in all groups by day 23 (Fig. 6a). The H&E staining indicated that the wound area was covered with epidermis and dermis, with some clear regeneration of skin appendages in the sprayed and unsprayed UC-MSCs group. In contrast, the wound area in the control group was covered with only a thin cell layer and few cells in the dermis (Fig. 6c). The Masson trichrome staining further confirmed that well-formed granulation tissue with appendages was regenerated in the sprayed and unsprayed groups, whereas only a thin layer of epidermis

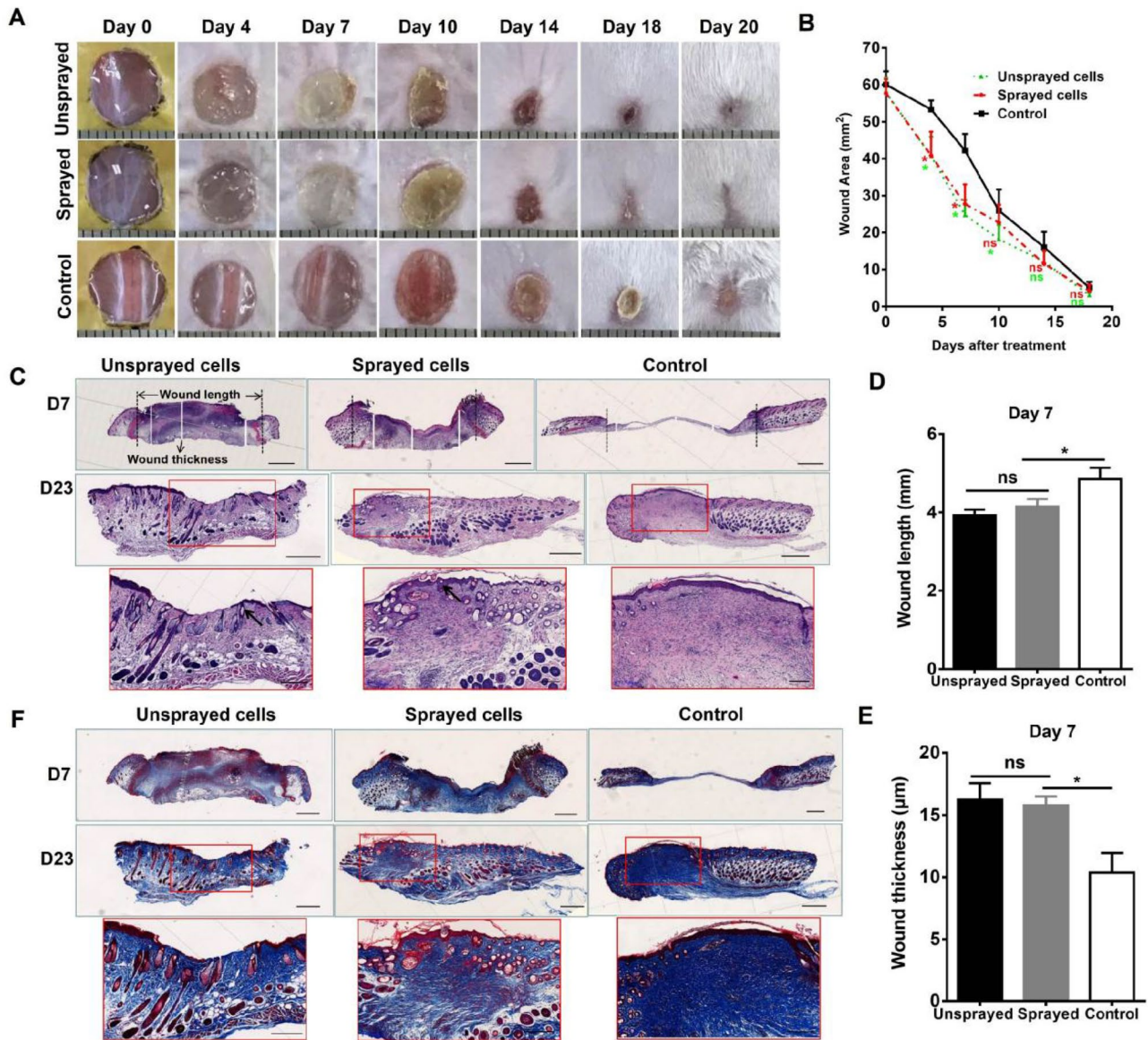


**Fig. 6** UC-MSCs sprayed by PAAD accelerated skin wound healing. **a** Representative images of the mouse wound treated with UC-MSCs (unsprayed), UC-MSCs sprayed by PAAD (sprayed) or control. **b** Analysis of changes in wound size (mm<sup>2</sup>) over time of the three groups showed that sprayed and unsprayed UC-MSCs significantly accelerated wound healing in the first 7 days.  $n=6$ . **c** Wound sections on day 7 and 21 post cell transplantation were stained with H&E for general observation of skin layers. Scale bar: 1 mm. Lower panels are magnified views of the red square. Scale bar: 200 µm. **d** Quantitative analysis on wound length on day 7 post transplantation showed sprayed and unsprayed UC-MSCs treated groups accelerated wound

healing comparing to control group. **e** Quantitative analysis showed skin thickness of sprayed and unsprayed groups were higher than that of the control group. **f** Trichrome staining showed collagen regeneration in the sprayed and unsprayed UC-MSCs application groups by day 7, while no collagen was seen in the control group. Epidermis and appendages were regenerated in sprayed and unsprayed UC-MSCs treated groups, while epidermis with minimal collagen deposition was found in the control. Scale bar: 1 mm. Lower panels are magnified views of the red squares. Scale bar: 200 µm. Numerical data represent means  $\pm$  SD. \* indicates  $p < 0.05$ , ns indicates  $p > 0.05$  versus the corresponding controls

with little granulation could be observed in the control group (Fig. 6f). Altogether, these results strongly suggest that the administration of sprayed UC-MSCs effectively recruited collagens and accelerated the skin healing process, indicating that the biological functions of UC-MSCs were well-maintained under the conditions of PAAD application.

### UC-MSCs sprayed by PAAD promotes wound re-epithelization

Immunofluorescent staining against CK14 (an epidermal progenitor cell marker) was applied to evaluate the re-epithelization effects of sprayed/unsprayed UC-MSCs. On day

7, no CK14-positive cells were found in the wound beds of either group (Fig. 7a). By day 23, re-epithelization had completed in all groups, however, CK14 staining was observed in both the epidermal layer and the skin appendages of animals treated with the sprayed and unsprayed cells, but only in the epidermal layer of control animals (Fig. 7a).

During the process of wound healing, epidermal cells migrate from the wound edge to the central wound area, thus forming a thin wedge-shaped epithelial tongue. The length of this epithelial tongue is therefore an index of re-epithelization. On day 14, CK14 staining indicated that an extensive epithelial tongue had spread into the wound center in the groups treated with sprayed and unsprayed UC-MSCs, but not in the control group (Fig. 7b). Quantitative analysis further revealed that the lengths of the epithelial tongues in both the sprayed and unsprayed UC-MSCs groups were significantly longer than those in the control ( $p < 0.05$ ), and there was no significant difference between the sprayed and the unsprayed group ( $p > 0.05$ ) (Fig. 7c). These observations suggest that the UC-MSCs sprayed by PAAD maintained their ability to promote re-epithelization during the process of wound repair.

## Discussion

Preclinical and clinical studies have equally shown that mesenchymal stem cells (MSCs) have the potential to treat chronic, non-healing wounds due to their regenerative, angiogenesis supportive, cytokine production and cell-recruiting properties [10, 12]. Over the past 30 years, cell application methods and cell delivery strategies were developed to achieve faster wound closure. However, due to the issues of decreased cell viability and function, the task of delivering cells efficiently and evenly into the wound bed has proven to be a prominent challenge in clinical practice.

Cells are traditionally transplanted intravenously, subcutaneously, or topically onto the wound surface area [34, 35]. Among these treatment forms, topical application onto the wound has been found to shorten treatment time and incur less pain for patients. This has prompted several designs of device for the spray application of cells to distribute them to the wound area quickly, homogeneously and without functional impairments, especially in cases of irregular, deep (into the dermis) or large-area skin wounds.

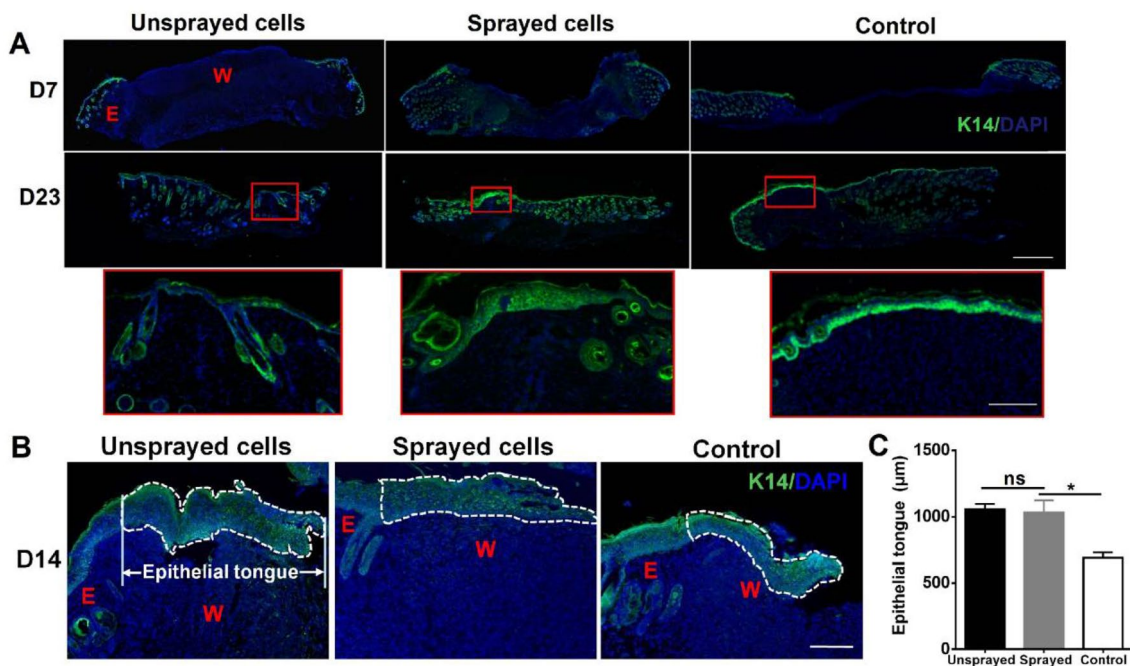


**Fig. 7** UC-MSCs sprayed by PAAD accelerated re-epithelialization of skin wound. **a** Immunofluorescent staining of CK14 in sections of wound skin showed no CK14<sup>+</sup> epidermal progenitors regenerated on day 7 after treatment in sprayed UC-MSCs, unsprayed UC-MSCs or saline-treated (control) groups. CK14<sup>+</sup> progenitors and appendages were regenerated in sprayed and unsprayed UC-MSCs treated groups on day 23, while no appendages were seen in the control. Scale bar: 1 mm. Lower panels are magnified views of the red squares. Scale

bar: 200 µm. E: wound edge, W: wound center. **b** On day 14, CK14 staining showed that epithelial tongues (circled area) migrated from the wound edge (E) into the wound center (W) in the sprayed UC-MSCs, unsprayed UC-MSCs or saline-treated (control) groups. **c** Quantitative analysis showed longer epithelial tongues in sprayed and unsprayed cells treated groups than those of the control group. Numerical data represent means  $\pm$  SD. \* indicates  $p < 0.05$ , ns indicates  $p > 0.05$  versus the corresponding controls

Sprayed cells are expected to suffer a certain level of damage during the aerosol process. Cell survival depends on many variables, such as the velocity of cell-containing droplets and the cell delivery pressure. By investigating cell viability and growth behavior immediately after aerosol delivery with an airbrush system [20], Veazey et al. found that cell viability significantly decreased with increasing pressure and decreasing nozzle diameter. In the same way, Fredriksson et al. observed an approximate 50% drop in viable cells immediately after transplantation when using a high-pressure device (200 kPa), and detected a further drop in viable cell numbers to nearly 40% after two weeks of culture [20]. Other studies investigated aerosol delivery by handheld airbrush systems with adjustable air pressure supply, and found that about 80% cell viability could be maintained under low delivery pressure (below 69 kPa) [20, 36].

Our data were consistent with the above observations, i.e., delivery pressure greatly affects the viability of sprayed cells. With the optimization of PAAD, the immediate viability of sprayed cells remained unaffected at air pressures under 80 kPa. Cell viability was shown to decrease to 90% at 90–100 kPa air pressure. Culturing cells sprayed under different air pressure values for 24 h showed that the proliferation of sprayed cells was well-retained only when the air pressure was under 70 kPa. These *in vitro* assays in conjunction with our preliminary data demonstrated that higher pressure provides more uniform droplets, thus we selected 70 kPa for subsequent experimental applications. Furthermore, the *in vitro* evaluation of biological functions indicated that sprayed primary cells retain their ability to form organoids in a 3D culture, and that the capacity for differentiation is unaffected. These results suggest that our newly designed PAAD can be safely used for both primary cells and cultured cell lines.

The PAAD designed in this study is intended specifically for the *in vivo* delivery of cells for wound healing. The findings of this study proved that, in comparison to the control group, the PAAD application of UC-MSCs accelerates wound closure and promotes the re-epithelialization and regeneration of skin appendages in a full-thickness excisional wound model. Given that collagen deposition serves as a scaffold necessary for re-epithelialization, and thus is a major function of UC-MSCs in wound healing, our results demonstrated that PAAD has considerable potential for clinical cell therapy, since sprayed UC-MSCs retained a strong capacity for collagen and fibronectin formation after the spray application. Moreover, the wound repair effects of the UC-MSCs sprayed by PAAD showed no significant impairment as compared to the unsprayed UC-MSCs, further evidencing that the biological function of UC-MSCs was well-maintained during the spraying process. Considering the fact that the wound in the animal experiments was rather small (0.8 cm<sup>2</sup>) and smooth, it can be inferred that the

clinical application of cell therapy with PAAD to treat deep and large wounds has the potential to achieve enhanced cell distribution and repair efficiency.

In fact, several cell spraying devices have been introduced in tissue repair and regeneration applications. For example, a bio-airbrush was developed for the treatment of cartilage defects to facilitate cartilage repair [23]. Devices for aerosolizing cell suspensions have been previously used to spray fibroblasts and keratinocytes on leg ulcers to accelerate healing [37, 38]; cell-spray auto-grafting technology was performed for deep partial-thickness burns [39]; and the aerosol spraying of bladder urothelial cells and smooth muscle cells was reported to reconstitute muscle segments for bladder augmentation [21]. In addition, cell-spray autografting was found to successfully enlarge the ratio of donor area to graft area from a routine 1:3 mesh to 1:100, thus facilitating operative therapy for larger deep burn areas [27, 40]. The migration and proliferation of keratinocytes from adjacent healthy epidermis to the wound site are essential steps during the skin wound healing process to facilitate re-epithelialization; MSCs were proven to promote this process in many reports [5, 10, 13], as well as in our study. As a major component of skin epidermis, keratinocytes seeded with scaffold materials have also been implicated in wound healing [41]. In the present study, we demonstrated that epidermal cells retain their organoid-forming capacity *in vitro*. In the future, an appropriate atomization method to deliver keratinocytes together with biomaterials using PAAD for wound therapy will be further explored. Correspondingly, we can foresee the potential for a wide adoption of the PAAD system for delivery of multiple cell types for repair and regeneration of different tissues and wound types.

## Conclusions

In this work, we presented a pneumatically assisted topical cell delivery device that can uniformly atomize cell suspensions at low air pressure. Results *in vitro* and *in vivo* both indicated that stem cell viability and function can be well-retained under optimal delivery settings. Moreover, the application of PAAD sprayed UC-MSCs in an animal wound model showed significant therapeutic effects, indicating a strong potential for the successful clinical adoption of this technique. It warrants mention that base membrane formation and rapid epithelialization are important considerations for the evaluation of novel cell sprays or carrier delivery methods [27, 42]. Future experiments aim to explore combination treatments using customized cell sources, such as mesenchymal cells and keratinocytes fixed in a PAAD-sprayable hydrogel matrix, to facilitate the better formation of dermal-epidermal junctions.

**Supplementary Information** The online version contains supplementary material available at <https://doi.org/10.1007/s42242-021-00144-5>.

**Acknowledgements** This work was funded by the Strategic Priority Research Program of the Chinese Academy of Sciences (No. XDA16020807), the Key Research and Development Program of Jiangsu Province, China (Nos. BE2018668 and BE2017669), the Major Innovative Research Team of Suzhou, China (No. ZXT2019007), SIBET and Jilin City Science and Technology Cooperation Project (No. E0550104), and Doctor of Entrepreneurship and Innovation Program of Jiangsu Province in the year of 2020.

**Author contributions** JZZ and SY designed the experiments. LXZ, XTY, LA, MJW, XX, and ZLM performed the experiments. LXZ drafted the manuscript. MTN and FZD performed the data analysis. JZZ and SY provided funding for this project and supervised the experiments. All authors approved the final manuscript.

## Declarations

**Conflict of interest** The authors declare that there is no conflict of interest.

**Ethical approval** All institutional and national guidelines for the care and use of laboratory animals were followed.

## References

- Gonzales KAU, Fuchs E (2017) Skin and its regenerative powers: an alliance between stem cells and their niche. *Dev Cell* 43(4):387–401. <https://doi.org/10.1016/j.devcel.2017.10.001>
- Tricco AC, Cogo E, Isaranuwatthai W et al (2015) A systematic review of cost-effectiveness analyses of complex wound interventions reveals optimal treatments for specific wound types. *BMC Med* 13:90. <https://doi.org/10.1186/s12916-015-0326-3>
- Wang Y, Beekman J, Hew J et al (2018) Burn injury: challenges and advances in burn wound healing, infection, pain and scarring. *Adv Drug Deliv Rev* 123:3–17. <https://doi.org/10.1016/j.addr.2017.09.018>
- Dimarino AM, Caplan AI, Bonfield TL (2013) Mesenchymal stem cells in tissue repair. *Front Immunol* 4:201. <https://doi.org/10.3389/fimmu.2013.00201>
- Tsai HW, Wang PH, Tsui KH (2018) Mesenchymal stem cell in wound healing and regeneration. *J Chin Med Assoc* 81(3):223–224. <https://doi.org/10.1016/j.jcma.2017.06.011>
- Bianco P, Robey PG, Simmons PJ (2008) Mesenchymal stem cells: revisiting history, concepts, and assays. *Cell Stem Cell* 2(4):313–319. <https://doi.org/10.1016/j.stem.2008.03.002>
- Baksh D, Yao R, Tuan RS (2007) Comparison of proliferative and multilineage differentiation potential of human mesenchymal stem cells derived from umbilical cord and bone marrow. *Stem Cells* 25(6):1384–1392. <https://doi.org/10.1634/stemcells.2006-0709>
- Yoo KH, Jang IK, Lee MW et al (2009) Comparison of immunomodulatory properties of mesenchymal stem cells derived from adult human tissues. *Cell Immunol* 259(2):150–156. <https://doi.org/10.1016/j.cellimm.2009.06.010>
- Secunda R, Vennila R, Mohanashankar AM et al (2015) Isolation, expansion and characterisation of mesenchymal stem cells from human bone marrow, adipose tissue, umbilical cord blood and matrix: a comparative study. *Cytotechnology* 67(5):793–807. <https://doi.org/10.1007/s10616-014-9718-z>
- Maxson S, Lopez EA, Yoo D et al (2012) Concise review: role of mesenchymal stem cells in wound repair. *Stem Cells Transl Med* 1(2):142–149. <https://doi.org/10.5966/sctm.2011-0018>
- Yan L, Zheng D, Xu RH (2018) Critical role of tumor necrosis factor signaling in mesenchymal stem cell-based therapy for autoimmune and inflammatory diseases. *Front Immunol* 9:1658. <https://doi.org/10.3389/fimmu.2018.01658>
- Maranda EL, Rodriguez-Menocal L, Badiavas EV (2017) Role of mesenchymal stem cells in dermal repair in burns and diabetic wounds. *Curr Stem Cell Res Ther* 12(1):61–70. <https://doi.org/10.2174/1574888x11666160714115926>
- Liu L, Yu Y, Hou Y et al (2014) Human umbilical cord mesenchymal stem cells transplantation promotes cutaneous wound healing of severe burned rats. *PLoS ONE* 9(2):e88348. <https://doi.org/10.1371/journal.pone.0088348>
- Xu Y, Hong Y, Xu M et al (2016) Role of keratinocyte growth factor in the differentiation of sweat gland-like cells from human umbilical cord-derived mesenchymal stem cells. *Stem Cells Transl Med* 5(1):106–116. <https://doi.org/10.5966/sctm.2015-0081>
- Rodriguez J, Boucher F, Lequeux C et al (2015) Intradermal injection of human adipose-derived stem cells accelerates skin wound healing in nude mice. *Stem Cell Res Ther* 6:241. <https://doi.org/10.1186/s13287-015-0238-3>
- Zeng RX, He JY, Zhang YL et al (2017) Experimental study on repairing skin defect by tissue-engineered skin substitute compositely constructed by adipose-derived stem cells and fibrin gel. *Eur Rev Med Pharmacol Sci* 21(3 Suppl):1–5
- Kim H, Hyun MR, Kim SW (2019) The effect of adipose-derived stem cells on wound healing: comparison of methods of application. *Stem Cells Int* 2019:2745640. <https://doi.org/10.1155/2019/2745640>
- Chang M, Liu J, Guo B et al (2020) Auto micro atomization delivery of human epidermal organoids improves therapeutic effects for skin wound healing. *Front Bioeng Biotechnol* 8:110. <https://doi.org/10.3389/fbioe.2020.00110>
- Falanga V, Iwamoto S, Chartier M et al (2007) Autologous bone marrow-derived cultured mesenchymal stem cells delivered in a fibrin spray accelerate healing in murine and human cutaneous wounds. *Tissue Eng* 13(6):1299–1312. <https://doi.org/10.1089/ten.2006.0278>
- Veazey WS, Anusavice KJ, Moore K (2005) Mammalian cell delivery via aerosol deposition. *J Biomed Mater Res B Appl Biomater* 72(2):334–338. <https://doi.org/10.1002/jbm.b.30159>
- Hidas G, Lee HJ, Bahoric A et al (2015) Aerosol transfer of bladder urothelial and smooth muscle cells onto demucosalized colonic segments for bladder augmentation: *in vivo*, long term, and functional pilot study. *J Pediatr Urol* 11(5):260. <https://doi.org/10.1016/j.jpuro.2015.02.020>
- Tritz J, Rahouadj R, DeIsla N et al (2010) Designing a three-dimensional alginate hydrogel by spraying method for cartilage tissue engineering. *Soft Matter* 6(20):3831–3835. <https://doi.org/10.1039/C000790K>
- Dijkstra K, Huitsing RPJ, Custers RJH et al (2019) Pre-clinical feasibility of the bio-airbrush for fully arthroscopic cell-based cartilage repair. *Tissue Eng Part C Methods* 25(7):379–388. <https://doi.org/10.1089/ten.TEC.2019.0050>
- Roberts A, Wyslouzil BE, Bonassar L (2010) Aerosol delivery of mammalian cells for tissue engineering. *Biotechnol Bioeng* 91(7):801–807. <https://doi.org/10.1002/bit.20549>
- Zimmerlin L, Rubin JP, Pfeifer ME et al (2013) Human adipose stromal vascular cell delivery in a fibrin spray. *Cytherapy* 15(1):102–108. <https://doi.org/10.1016/j.jcyt.2012.10.009>
- Beneke V, Küster F, Neehus AL et al (2018) An immune cell spray (ICS) formulation allows for the delivery of functional monocyte/macrophages. *Sci Rep* 8(1):16281. <https://doi.org/10.1038/s41598-018-34524-2>

27. Horst BT, Chouhan G, Moiemmen NS et al (2018) Advances in keratinocyte delivery in burn wound care. *Adv Drug Deliv Rev* 123:18–32. <https://doi.org/10.1016/j.addr.2017.06.012>
28. Fredriksson C, Kratz G, Huss F (2008) Transplantation of cultured human keratinocytes in single cell suspension: a comparative *in vitro* study of different application techniques. *Burns* 34(2):212–219. <https://doi.org/10.1016/j.burns.2007.03.008>
29. Xie Y, Li Y (2010) Experimental study of human umbilical cord mesenchymal stem cell isolation, culture and biological characteristics. *J Bengbu Med College* 10:982–985. <https://doi.org/10.13898/j.cnki.issn.1000-2200.2010.10.005>
30. Jensen KB, Driskell RR, Watt FM (2010) Assaying proliferation and differentiation capacity of stem cells using disaggregated adult mouse epidermis. *Nat Protoc* 5(5):898–911. <https://doi.org/10.1038/nprot.2010.39>
31. Yang R, Liu F, Wang J et al (2019) Epidermal stem cells in wound healing and their clinical applications. *Stem Cell Res Ther* 10(1):229. <https://doi.org/10.1186/s13287-019-1312-z>
32. Boonekamp KE, Kretzschmar K, Wiener DJ et al (2019) Long-term expansion and differentiation of adult murine epidermal stem cells in 3D organoid cultures. *PNAS* 116(29):14630–14638. <https://doi.org/10.1073/pnas.1715272116>
33. Darby IA, Hewitson TD (2007) Fibroblast differentiation in wound healing and fibrosis. *Int Rev Cytol* 257:143–179. [https://doi.org/10.1016/S0074-7696\(07\)57004-X](https://doi.org/10.1016/S0074-7696(07)57004-X)
34. Duscher D, Barrera J, Wong VW et al (2016) Stem cells in wound healing: the future of regenerative medicine? A mini-review *Gerontology* 62(2):216–225. <https://doi.org/10.1159/000381877>
35. Kirby GTS, Mills SJ, Cowin AJ et al (2015) Stem cells for cutaneous wound healing. *Biomed Res Int* 2015:285869. <https://doi.org/10.1155/2015/285869>
36. Hendriks J, Visser CW, Henke S (2015) Optimizing cell viability in droplet-based cell deposition. *Sci Rep* 5:11304. <https://doi.org/10.1038/srep11304>
37. Kremer M, Lang E, Berger AC (2000) Evaluation of dermal—epidermal skin equivalents ('composite-skin') of human keratinocytes in a collagen-glycosaminoglycan matrix (integra™ artificial skin). *Br J Plast Surg* 53(6):459–465. <https://doi.org/10.1054/bjps.2000.3368>
38. Kirsner RS, Marston WA, Snyder RJ et al (2012) Spray-applied cell therapy with human allogeneic fibroblasts and keratinocytes for the treatment of chronic venous leg ulcers: a phase 2, multi-centre, double-blind, randomised, placebo-controlled trial. *Lancet* 380(9846):977–985. [https://doi.org/10.1016/S0140-6736\(12\)60644-8](https://doi.org/10.1016/S0140-6736(12)60644-8)
39. Esteban-Vives R, Choi MS, Young MT et al (2016) Second-degree burns with six etiologies treated with autologous noncultured cell-spray grafting. *Burns* 42(7):e99–e106. <https://doi.org/10.1016/j.burns.2016.02.020>
40. Esteban-Vives R, Corcos A, Choi MS et al (2018) Cell-spray autografting technology for deep partial-thickness burns: problems and solutions during clinical implementation. *Burns* 44(3):549–559. <https://doi.org/10.1016/j.burns.2017.10.008>
41. Kobayashi J, Kikuchi A, Aoyagi T et al (2019) Cell sheet tissue engineering: cell sheet preparation, harvesting/manipulation, and transplantation. *J Biomed Mater Res A* 107(5):955–967. <https://doi.org/10.1002/jbm.a.36627>
42. Butler CE, Orgill DP (2005) Simultaneous *in vivo* regeneration of neodermis, epidermis, and basement membrane. *Adv Biochem Eng Biotechnol* 94:23–41. <https://doi.org/10.1007/b99998>